Available online at www.sciencedirect.com
ScienceDirect
Journal of Crystal Growth 303 (2007) 80–84
JOURNAL OF CRYSTAL GROWTH
www.elsevier.com/locate/jcrysgro

Step meandering in epitaxial growth

Frank Haußer[a,*], Axel Voigt[a,b]

[a]Crystal Growth Group, Research Center caesar, Ludwig-Erhard-Allee 2, 53175 Bonn, Germany
[b]Institut für wissenschaftliches Rechnen, Technische Universität Dresden, Zellescher Weg 12-14, 01062 Dresden

Available online 25 January 2007

Abstract

We present theoretical investigations of meandering dynamics on vicinal surfaces during MBE growth. Our results are based on the numerical simulation of a step flow model, which accounts for asymmetric attachment/detachment kinetics at the steps. In the long wave regime, where the meander wavelength is large compared to the terrace width, our simulations of the full model confirm the results of Pierre-Louis et al. [Phys. Rev. Lett. 80 (1998) 4221; Phys. Rev. E 68 (2003) 020601; J. Crystal Growth 275 (2005) 56], based on a local amplitude equation: we observe meandering with a wavelength being determined by the linear instability in the early stage, and endless growth of the amplitude; in the presence of anisotropic edge energy, interrupted coarsening does take place. When passing to shorter wavelengths we reveal two other types of nonlinear dynamics: (a) mushroom formation and subsequent pinch-off leading to a vacancy island, and (b) emerging of a stationary step profile with fixed amplitude.

PACS: 68.55.Ac; 81.10.Aj; 05.45.−a

Keywords: A1. Growth models; A1. Morphological instability; A3. Ehrlich-Schwoebel effect; A3. Epitaxial growth; A3. Molecular beam epitaxy

1. Introduction

Epitaxial growth is an important technological process to produce high quality crystalline films. The engineering of small structure, e.g. for modern electronic devices demands control over such films down to a thickness of only some atomic layers. It is well known, that the morphology of such films grown by various epitaxial growth techniques is subject to instabilities. An understanding of these instabilities in realistic growth scenarios is therefore of utmost importance if films with prescribed properties have to be produced.

There are essentially three types of instabilities which influence the film morphology during growth: step bunching, step meandering and mound formation, see, e.g. [1,2]. Here we will concentrate on step meandering, as a result of a terrace Ehrlich–Schwoebel (ES) barrier [3]. A fundamental result of the linear stability analysis of Ref. [4] is the prediction for the meander wavelength in the initial stage of the instability. For practical purposes, however, the nonlinear regime of the instability is of much more importance, because meandering patterns observed during growth show large amplitudes.

In this work the nonlinear regime will be investigated by solving the mesoscopic step flow model [5] numerically for a periodic sequence of steps. If the meander wavelength is large compared to the terrace width, we observe meandering with a wavelength being determined by the linear instability in the early stage, and endless growth of the amplitude as $\sqrt{t}$. In the presence of anisotropic edge energies this is no longer true and the wavelength might change during growth. Coarsening does take place in an intermediate stage, whereas in the late stage the coarsening stops. These findings compare very well with the results obtained by Refs. [6–8], where a local amplitude equation for the step profile has been derived and used to investigate the nonlinear meander evolution.

Our main result concerns the regime, in which the local amplitude equation is not valid anymore: passing to shorter meander wavelength being of similar size as the terrace width, the step profile starts to develop overhangs,

*Corresponding author. Tel.: +49 228 9656 272; fax: +49 228 9656 187.
E-mail address: hausser@caesar.de (F. Haußer).

0022-0248/$ - see front matter © 2006 Elsevier B.V. All rights reserved.
doi:10.1016/j.jcrysgro.2006.11.149

which eventually lead to a self-crossing of the steps and thus to the formation of a closed loop, i.e. a vacancy island—a void of the depths of one atomic height. If the steps become even more isolated, i.e. if the meander wavelength is considerably smaller than the terrace width, we observe stationary step profiles with a fixed amplitude.

We note, that the formation of vacancy islands has also been observed in kinetic Monte-Carlo simulations of a standard SOS model on a square lattice in Ref. [9]. In this work, however, a parameter regime, where the Kink–ES effect is the main reason for the meander instability, has been investigated.

The paper is organized as follows: in Section 2, we describe the model, in Section 3, we present and discuss our results in the linear and nonlinear regime, and in Section 4 we draw conclusions.

2. Step flow model

We recall the classical Burton–Cabrera–Frank (BCF) model. The adatom density c on the terraces obeys the following diffusion equation:

$$\partial_t c + \nabla \cdot \vec{j} = F, \quad \vec{j} = -D\nabla c, \tag{1}$$

where D is the diffusion constant and F is the deposition flux rate. Desorption of adatoms has been neglected, which is valid in typical MBE experiments [10,11]. The fluxes of adatoms to a step are given by

$$j_\pm := \pm \vec{j}_\pm \cdot \vec{n} - c_\pm v, \tag{2}$$

where subscripts $+,-$ denote quantities at the upper and lower terrace, respectively, $\vec{n}$ denotes the normal pointing from upper to lower terrace and v is the normal velocity of the step. Assuming first order kinetics for the attachment/detachment of adatoms at the steps, the adatom density satisfies the following kinetic boundary conditions at a step:

$$j_\pm = k_\pm(c_\pm - c_{\mathrm{eq}}). \tag{3}$$

With this notation, asymmetric attachment rates $0 < k_+ < k_-$ model the (terrace) ES effect. The equilibrium density c_{eq} is given by the linearized Gibbs–Thomson relation

$$c_{\mathrm{eq}} = c^*(1 + \Gamma\kappa), \quad \Gamma = \Omega(\gamma + \gamma'')/(k_{\mathrm{B}}T),$$

where $\Omega = a^2$ is the atomic area, a being the lattice spacing. Finally, the normal velocity of a step is given by

$$v = \Omega(j_+ + j_-) + a\partial_s j_s, \quad j_s = -D_{\mathrm{st}}\partial_s(\Gamma\kappa), \tag{4}$$

where ∂_s denotes the tangential derivative along the step and D_{st} is the diffusion constant of atoms along the step. The second term in the velocity law (4) represents edge diffusion of edge atoms along the step, whereas the first term ensures mass conservation.

3. Results

The results below were obtained using numerical simulations of the full free boundary problem as defined by Eqs. (1)–(4). A front tracking method based on linear adaptive finite elements is used, see Ref. [12].

The parameters are given in dimensionless units and have to be rescaled to obtain the physical units. For the parameters used in the examples below, one should use a spatial unit $\bar{x} \sim 10a - 100a$ and a temporal unit $\bar{t} \sim 10^{-2}\,\mathrm{s} - 10^{-4}\,\mathrm{s}$ to obtain reasonable physical parameters. All results will be stated in terms of the time unit ML (monolayer) and the space unit defined by the most unstable wavelength λ_m of the linear instability.

3.1. Linear instability

Since the seminal work of Bales and Zangwill [4] it is well known, that the (terrace) ES barrier ($k_+ < k_-$) does lead to a linear instability of a step meander. Here, the in-phase mode is most prominent and the growth rate $\omega(k)$ of a step train depending on the wave number k has been given explicitly in Ref. [4]. For the in-phase mode and if the meander wavelength is much larger than the interterrace distance l, i.e. $kl \ll 1$, it reads

$$\omega(k) = \tfrac{1}{2}\Omega F l^2 f_{\mathrm{ES}} k^2 - \Gamma(c^*\Omega D l + aD_{\mathrm{st}})k^4, \tag{5}$$

where (denoting $d_\pm = D/k_\pm$)

$$f_{\mathrm{ES}} = \frac{d_+ - d_-}{d_+ + d_- + l} \tag{6}$$

does measure the strength of the ES effect. In this approximation, the most unstable wavelength λ_{m} is explicitly given by

$$\lambda_{\mathrm{m}} = 4\pi\left(\frac{\Gamma(c^*\Omega D l + aD_{\mathrm{st}})}{\Omega F l^2 f_{\mathrm{ES}}}\right)^{1/2}.$$

In the general case, i.e. not assuming $kl \ll 1$, the dispersion relation (5) becomes more complicated [4] and there is no explicit formula for the most unstable wavelength.

We first use the linear instability to validate the numerical scheme. To this end we consider a periodic step train modeled as two down steps with terrace width $l = 10$ on a periodic domain of size 100×20. Using the parameters $D = 10^2$, $c^* = 10^{-3}$, $k_+ = 1$, $k_- = 10$, $\Gamma = 10$, $D_{\mathrm{st}} = 0$ and $F = 2 \times 10^{-3}$, the predicted most unstable wavelength is $\lambda_{\mathrm{m}} \approx 100$. In the numerical simulations, the randomly perturbed steps synchronize very fast and then develop the predicted meander with a growth rate coinciding very well with the theoretical dispersion relation, see Fig. 1. We also note, that in all numerical tests with a larger number of equally spaced steps, the step meander synchronized at an early stage of the evolution. Thus, it is sufficient to simulate the evolution of two steps on a periodic domain to investigate the meandering instability in the nonlinear regime.

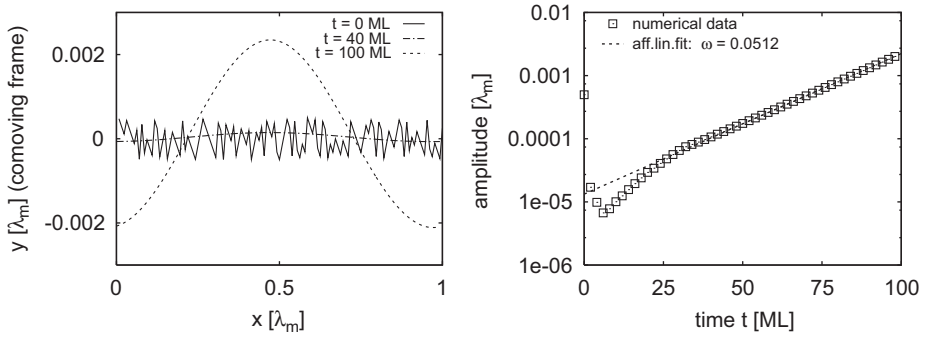

Fig. 1. Time evolution of two equidistant, initially straight steps with small-amplitude random perturbation on a periodic domain. (Left) Profile of one of the two steps at different times shows the emergence of a meander instability with a wavelength corresponding to the most unstable wavelength of the linear instability. (Right) The predicted growth rate $\omega(\lambda_m) = 0.0516(\mathrm{ML})^{-1}$ compares very well with the numerically obtained value $\omega = 0.0512(\mathrm{ML})^{-1}$.

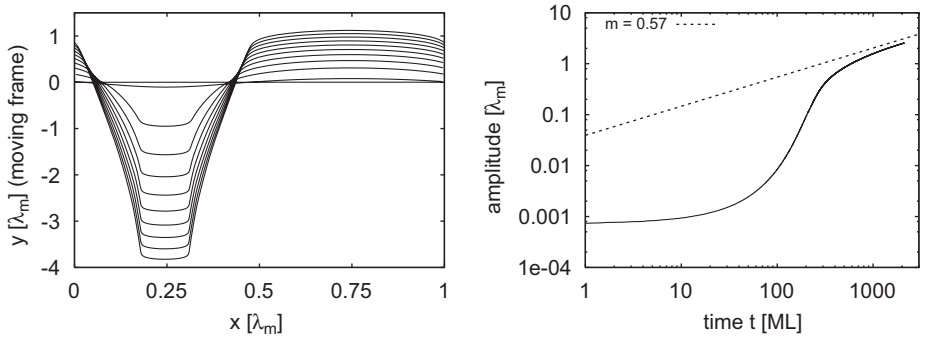

Fig. 2. Evolution of a step meander in the long wavelength regime $l/\lambda_m = 0.1$. (Left) Profile of a step (moving upwards) at different times depicted in a co-moving frame. One observes endless growth of the amplitude, a symmetry breaking between the forward and the backward meander in the nonlinear regime and the emerging of plateaus. (Right) The meander amplitude grows approximately as $\sqrt{t}$ in the late stage.

3.2. Long wavelength regime

Having validated the numerical method with the linear instability, we next turn to the nonlinear evolution. Assuming that the meander wavelength λ_m is much larger than the interterrace distance l, an expansion in the small parameter $\varepsilon := (l/\lambda_m)^2$ leads to a (highly nonlinear) local evolution equation for the amplitude $\xi = \xi(x, t)$ of a single step meander (step profile) in a periodic, synchronized step train, see Refs. [6–8]. However, it is not clear from the beginning, whether and to what extend the local evolution equation is also valid, when the amplitudes of the meander become large. Therefore, we compare with the simulations of the full model.

In Fig. 2 the meandering of a step using the full model is shown. Here the parameters have been chosen such that $l/\lambda_m = 0.1$. One observes endless growth of the amplitude, a symmetry breaking between the forward and the backward meander in the nonlinear regime and the emerging of plateaus. Moreover, the increase of the meander amplitude approaches $\sim\sqrt{t}$ in the late stage. These findings confirm the predictions made in Refs. [6,13,8], based on the local amplitude equation. We also confirm for the full model, that no coarsening appears for isotropic edge energies, whereas for anisotropic edge energies interrupted coarsening can be observed, see Fig. 3, in agreement with [7].

Summarizing, the numerical simulations of the full model confirm, that the local evolution equation [6–8] captures the main properties of the step flow model in the long wavelength regime.

3.3. Crossover to short wavelength regime

When passing to the regime where the meander wavelength λ_m and the terrace width l become comparable in size, the local amplitude equation is not valid anymore. Thus, one might expect a rather different behavior of the evolution of a step meander in the nonlinear regime. Indeed our numerical simulations reveal, that the nonlinear dynamics changes drastically, see Fig. 4: when passing to shorter wavelengths, the step profile starts to develop overhangs (“mushroom formation”), which still allow for endless growth of the amplitudes (of the periodic step train), see Fig. 4(a,b). Further decreasing the meander wavelength (while keeping the terrace width fixed) leads to a pinch-off, i.e. the formation of a vacancy island as shown in Fig. 4(c). As soon as the self-intersection of the step profile occurs, the simulation based on a front-tracking method does stop. Finally, we observe the appearance of a

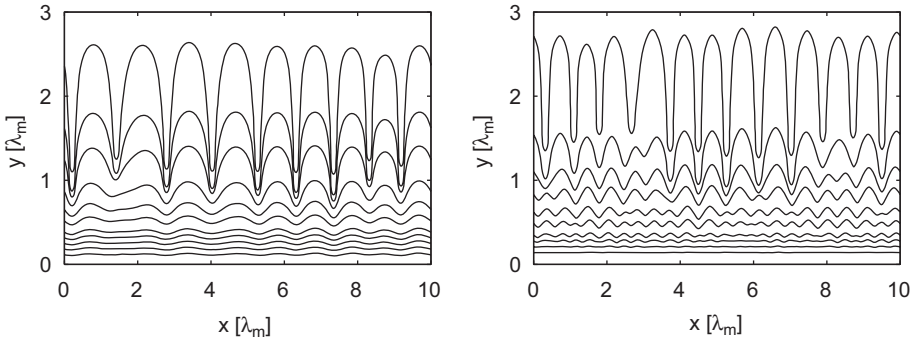

Fig. 3. Meandering on a larger domain of size $10\lambda_m$, λ_m being the most unstable wavelength in the isotropic case. (Left) Isotropic edge energy: the wavelength is fixed in the initial stage followed by endless growth of the amplitude. (Right) Anisotropic edge energy leads to $\Gamma(\theta) = \Gamma_0(1 + 0.9\cos(4(\theta - \pi/4)))$: after selection of the most unstable wavelength (being smaller as in the isotropic case, since $\Gamma(\theta = 0) < \Gamma_0$), one observes coarsening in the intermediate stage. In the late stage, the coarsening stops.

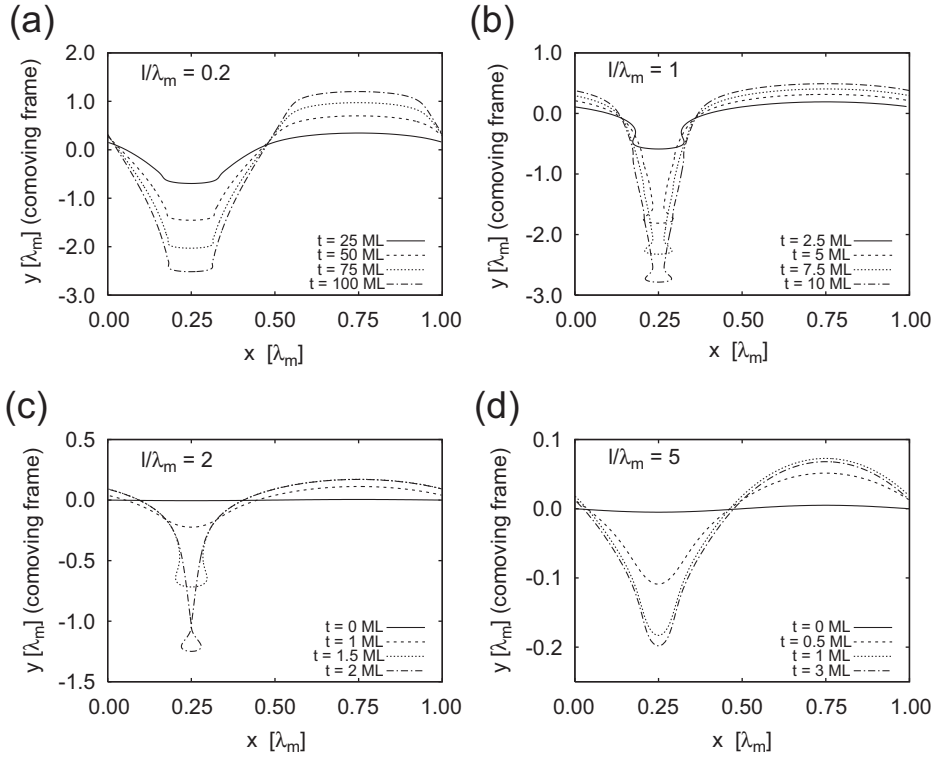

Fig. 4. Evolution of a step meander; crossover to large l/λ_m. For intermediate $l/\lambda_m \approx 1$ the step profile starts to develop overhangs, but we still observe endless growth of the amplitude, see (a),(b). Further increase of l/λ_m leads to a pinch-off, i.e. the formation of a vacancy island as shown in (c). For even larger l/λ_m the step profile evolves to a steady state with a finite amplitude, see (d). The following parameters have been used in the simulations: $k_+ = 1$, $k_- = 100$, $F = 10^{-3}$, $D = 10^2$, $c^* = 10^{-3}$, $D_{st} = 0$, $l = 10$. The most unstable wavelength λ_m (and therefore the ratio l/λ_m) is varied by changing the stiffness Γ from $\Gamma = 1.4$ to 10^{-3}.

steady state step profile, if the wavelength is even further decreased.

4. Conclusion

Using numerical simulations of the full step flow model consisting of the adatom diffusion equation on the terraces, asymmetric attachment kinetics at the steps and a velocity law for the movement of the steps we have investigated the morphological instability caused by the ES effect. In the long wave regime, where the meander wavelength is large compared to the terrace width, our results confirm that the essential features of the nonlinear behavior may be captured by the local amplitude equation as obtained in Refs. [6,7]. Passing to regimes, where the meander wavelength and the terrace width are comparable in size we find a crossover from endless growth to mushroom formation with subsequent pinch-off resulting in vacancy

islands. Even more interestingly, upon further decreasing the meander wavelength, we find steady state meander with a fixed amplitude. We note that passing from large to small meander wavelength (while keeping the terrace width fixed) causes the steps to be more isolated, which may be an explanation, why mushroom formation becomes possible.

Acknowledgments

We thank O. Pierre Louis for valuable discussions. FH has been partially supported by BMBF, through 03VGNKVB. AV has been partially supported by EU FP6, through NMP STRP 016447 "MagDot".

References

[1] P. Politi, G. Grenet, A. Marty, A. Ponchet, J. Villain, Phys. Rep. 324 (2000) 271.
[2] J. Krug, in: A. Voigt (Ed.), Multiscale Modeling of Epitaxial Growth, ISNM, vol. 149, Birkhäuser, Basel, 2005.
[3] R.L. Schwoebel, J. Appl. Phys. 40 (1969) 614.
[4] G.S. Bales, A. Zangwill, Phys. Rev. B 41 (1990) 5500.
[5] W.K. Burton, N. Cabrera, F.C. Frank, Philos. Trans. R. Soc. London Ser. A 243 (866) (1951) 299.
[6] O. Pierre-Louis, C. Misbah, Y. Saito, J. Krug, P. Politi, Phys. Rev. Lett. 80 (1998) 4221.
[7] G. Danker, O. Pierre-Louis, K. Kassner, C. Misbah, Phys. Rev. E 68 (2003) 020601.
[8] O. Pierre-Louis, G. Danker, J. Chang, K. Kassner, C. Misbah, J. Crystal Growth 275 (2005) 56.
[9] J. Kallunki, J. Krug, Europhys. Lett. 66 (5) (2004) 749.
[10] T. Maroutian, L. Douillard, H.J. Ernst, Phys. Rev. Lett. 83 (1999) 4353.
[11] T. Maroutian, L. Douillard, H.J. Ernst, Phys. Rev. B 64 (2001) 165401.
[12] E. Bänsch, F. Haußer, O. Lakkis, B. Li, A. Voigt, J. Comput. Phys. 194 (2004) 409.
[13] F. Gillet, O. Pierre-Louis, C. Misbah, Eur. Phys. J. B 20 (2000) 519.